Plant root penetration and growth as a mechanical inclusion problem

B. Calusi [a,b,*,**], F. Tramacere [a], S. Gualtieri [a], N.M. Pugno [b,c,d,**], B. Mazzolai [a,**]

[a] *Center for Micro-BioRobotics, Istituto Italiano di Tecnologia, Viale Rinaldo Piaggio 34, 56025 Pontedera, Italy*
[b] *Laboratory of Bio-inspired & Graphene Nanomechanics, Department of Civil, Environmental and Mechanical Engineering, University of Trento, Via Mesiano 77, 38123 Trento, Italy*
[c] *Ket-Lab, Amaldi Foundation, Via del Politecnico snc, 00133 Rome, Italy*
[d] *School of Engineering and Materials Science, Queen Mary University of London, Mile End Road, London E1 4NS, UK*

A B S T R A C T

The ability of plant roots to penetrate soils is affected by several stimuli exerted by the surrounding medium, such as mechanical stresses and chemical stimuli. Roots have developed different adaptive responses, such as increase or decrease of the elongation rate of the apical region and swelling or shrinking of its diameter. We propose a mathematical model aimed at explaining the dynamic evolution of plant roots during the penetration into the soil. We treat the root as a cylinder and the root–soil interaction as a purely mechanical inclusion problem. In particular, the root dynamic evolution is based on a modified version by one of the authors of the extended universal law of West, Brown, and Enquist. Coupling the solution of the mechanical problem and the growth equation, we compare the theoretical results with experimental data collected in artificial and real soils. In this work, we propose a plausible interpretation of the experimental results of the root behavior during the growth inside the surrounding soil medium.

1. Introduction

Plants do not follow a rigid predefined growing plan but adjust their strategy to environmental conditions. Upon germination, plant architecture is driven by a genetic post-embryonic program, which is at the basis of the plant plasticity [1,2]. The study in [3] identified two types of plant plasticity based on morphological or physiological mechanisms. Morphological mechanisms require high energetic costs because new functional portions are produced. On the other hand, in the physiological mechanism, the modifications occurring in differentiated tissue are imperceptible, the process is completely reversible and the energetic cost is very low. The two types of plasticity are continuously expressed during plant life since they are fundamental for their own survival [4]. The root architecture is led by the root tip, which has the entire control of the root structure in the space of a few millimeters [5]. Therefore, roots adapt to the dynamically changing soil features, mainly its impedance, with several responses, such as the shrinking of the diameter, the root-structure architecture modification, mucus secretion [6–9], affecting in turn the surrounding medium (Fig. 1). Several investigations to understand how plant roots can modulate and control the external stimuli on their growth have been performed [10–16]. Typically, a growing plant root can exert an estimated maximum pressure up to 1 MPa [17] and, consequently, can arrest its growth when the pressure required to penetrate the

soil is higher than such threshold value. For maize root, the arrest of the growth has been reported with a penetration resistance of 0.8–2 MPa [18,19], and in [9] some maize plants did not grow beyond a penetration resistance of 0.25 MPa. The growth pressure is defined as the stress, acting normally at the root surface, which a root has to exert in order to deform the soil around it. Although a penetrometer probe is widely used to estimate the pressure that a root has to exert for penetrating soils, the studies in [17] and [19] demonstrated that this procedure overestimates the root growth strength. In literature, growth models for plant roots are mainly based on Lockhart's equation [20–24]. To better understand root penetration strategies and phenomena involved in this process, the investigation of key parameters is required. One option is to investigate penetration mechanisms and adaptation through mathematical modeling and experimental techniques. In particular, many experimental studies illustrated the evolution of root system in nutrient-rich patches [25–29] analyzing phenotypical reactions (branching, root elongation, lateral root emergence, root hairs proliferation, etc.). Since the majority of these studies were conducted in real soils [30,31], characterized by high heterogeneity, these findings have to be considered as a result of several physical and chemical stimuli. In fact, in order to properly investigate each phenomenon and carry out a rigorous cause–effect analysis, plants should be studied in environments that allow to distinguish each single stimulus. In order to

---

* Currently at the: Istituto Nazionale di Geofisica e Vulcanologia, Via Cesare Battisti 53, 56125 Pisa, Italy.
** Corresponding authors.
  E-mail addresses: benedetta.calusi@ingv.it (B. Calusi), nicola.pugno@unitn.it (N.M. Pugno), barbara.mazzolai@iit.it (B. Mazzolai).
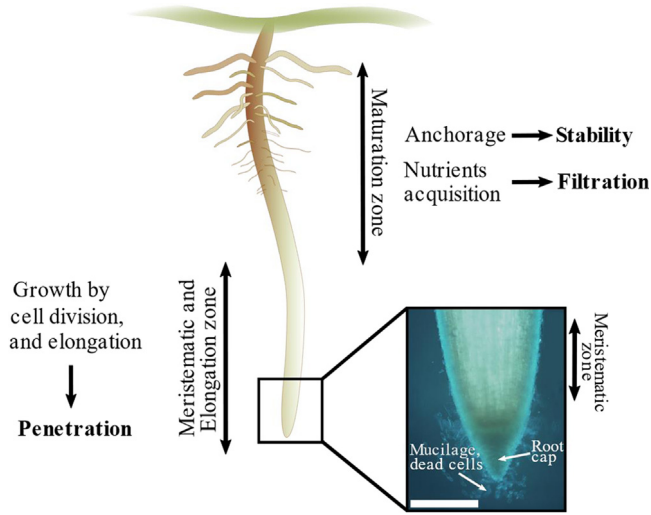
Fig. 1. Schematic diagram of the plant root structure. The growth phenomenon occurs at the apical region through cell growth and elongation. The growing region is constituted by the elongation zone and the meristem. Therefore, the growing tip with mucilage and cell secretion at the root cap enables the root penetration into the soil. The maturation zone is stationary and it is characterized by the presence of lateral hairs on the roots. The presence of hairs and lateral roots in the mature zone provides nutrients acquisition and anchorage. Scale bar is 500 μm.

Fig. 2. Diagram of the domain for the embedded elastic cylinder and the surrounding elastic matrix. The zooms show the inclusion problem applied to the domain related to the tip region of the elastic cylinder, C, of radius R and length L. Such zone is subjected to axial, $\bar{p}$, and radial pressure, p. The corresponding surrounding matrix, M, is such that $M = C^+ \cup C^-$ with the cylindrical hole (with radius R_1 and length L_1) subjected to axial, $\bar{p}$, and radial pressure, p. The matrix M has length L_2 and radius R_2, respectively.

discriminate indiscernible parameters in a real environment [32], we investigated the growth of plant roots in artificial soils with different soil and nutrient concentrations in the absence of other physical or chemical stimuli.

Therefore, in this work, to shed light on the conducted experimental results we propose a mathematical model. The mathematical model is based on an elastic inclusion problem to investigate the growth of plant root and its surrounding medium. In fact, the field of mechanics seems to have a prominent role to investigate and explain biomechanical mechanisms [33–36]. In particular, the theory of linear elasticity can offer a possible way to describe complex processes by translating into mechanical problems, such as the brain deformation due to a decompressive craniectomy [35] and the mechanical relationship between the tumor growth and its environment [33,34]. In this regard, we studied the mechanical inclusion of a finite cylinder into a cylinder of infinite length as a highly idealized system of the interaction between the growing root and the surrounding soil medium. By exploiting a continuum mechanics approach, we treated the plant root as an elastic cylinder and the soil as a homogeneous elastic fracturable matrix, in agreement with [33]. Since we focused on the variation of the root elongation caused by the interactions with the surrounding environment, we considered a single isolated root growing in the axial direction. We applied our model in the specific case of *Zea mays* primary root growth in artificial soil with different concentration of Phytagel and in real soils with different soil compactness. In addition, we extended our model to describe experiments conducted in Phytagel medium with the presence of an excessive Murashige and Skoog Basal Salt Mixture concentration to test the influence on both the root elongation and radial expansion. The paper is organized as follows. A description of the formulation of the inclusion problem is given in Section 2. Section 3 describes the root growth in the case of (1) axial expansion assuming the absence of nutrients in the surrounding medium; (2) axial and radial expansion considering the presence of nutrients in the soil medium. Sections 4 and 5 summarize the results and concluding remarks, respectively.

Our approach introduces certain simplification to model the complex interaction between the root and the surrounding soil medium. Therefore, we disregarded some mechanisms involved in the phenomenon of root growth into the soil medium, e.g. the flow at the root–soil interface.
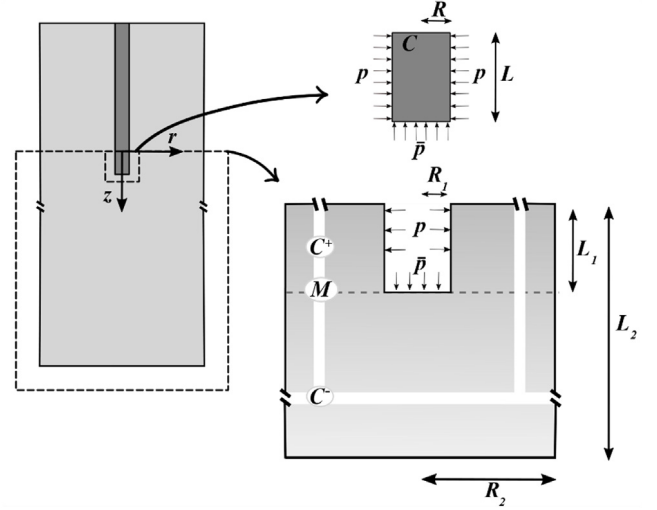
2. Preliminaries and problem formulation

We focus on biological phenomena in which the time-scale of growth is longer than the time-scale of the elastic response, this latter is hypothesized as being a quasi-static phenomenon, thus inertial forces are negligible. We consider the problem of the inclusion of a cylinder in a matrix. We treat both the cylinder and the matrix as linearly elastic, homogeneous, and isotropic material. The constitutive relationship between the stress tensor $\{\sigma_{ik}\}_{i,k}$ and the strain tensor $\{\epsilon_{ik}\}_{i,k}$ is given by [37,38]

$$\sigma_{ik} = \frac{E}{1+\nu}\left(\epsilon_{ik} + \frac{\nu}{1-2\nu}\epsilon_{ll}\delta_{ik}\right),$$

where E and ν are the Young's modulus and Poisson's ratio of the material. The strain tensor can be written as a function of the displacement vector $\boldsymbol{u}$

$$\epsilon_{ik} = \frac{1}{2}\left(u_{k,i} + u_{i,k}\right).$$

By introducing cylindrical coordinates (r, θ, z), we assume that the displacement vector is

$$\boldsymbol{u}(r,\theta,z) = \left(u_r, u_\theta, u_z\right) = \left(u_r(r), 0, u_z(z)\right). \tag{1}$$

For Eq. (1) the non-vanishing components of the strain tensor are $\epsilon_{rr} = u_{r,r}$, $\epsilon_{\theta\theta} = u_r/r$, $\epsilon_{zz} = u_{z,z}$. According to the assumption of steady-state process, the equilibrium equation is

$$2(1-\nu)\nabla(\nabla \cdot \boldsymbol{u}) - (1-2\nu)\nabla \times (\nabla \times \boldsymbol{u}) = 0. \tag{2}$$

In order to describe the plant root growth as an inclusion problem, we assume that the growing phenomenon involves only the tip region of the embedded cylinder. We denote the domain of the growing zone C, the surrounding matrix as M, and we split M into two subdomains $C^+, C^-, C^+ \cup C^- = M$ as in Fig. 2. Therefore, we assume that the growing domain, C, is cylindrical, with radius R and length L, and that the growth occurs only in the axial direction. The cylinder is closed at both ends and subjected to the outer pressure $\bar{p}$ on the bottom surface at $z = L$ and p in the radial direction. The upper part of the matrix is a linear elastic isotropic thick-walled cylinder, C^+, of inner and outer radii R_1 and R_2, respectively. p is the pressure applied at R_1. We then consider a linear elastic isotropic cylinder, C^-, of radius R_2. We suppose

that the cylinder C^- is closed at the bottom end (at $z = L_2$) and the top end is subjected to axial pressure $\bar{p}$ over a circle of radius R_1. In order to meet the experimental conditions, we require that there is no displacement over the whole outer surface of M. First, we compute stresses and displacements in the elastic matrix, M, with a cylindrical hole, and then in the elastic cylinder, C. In the case of the elastic matrix, Eq. (2) has the following solution[1]

$$
\begin{cases}
u_r^+ (r) = \dfrac{C_1^+ r}{2} + \dfrac{C_2^+}{r} & in\ C^+, \\[2mm]
u_z^+ (z) = C_3^+ z + C_4^+ & in\ C^+, \\[2mm]
u_r^- (r) = \dfrac{C_1^- r}{2} & in\ C^-, \\[2mm]
u_z^- (z) = C_3^- z + C_4^- & in\ C^-,
\end{cases}
$$

where u^+, u^- are the displacements of the upper and lower part of the matrix, respectively. Thus, we look for values of the constants such that the following boundary conditions

$$
\begin{cases}
\sigma_{rr}^+ = -p & r = R_1, z \in (0, L_1), \\
u_r^+ (R_2) = 0 & z \in (0, L_1), \\
u_r^+ (R_2) = 0 & z \in (L_1, L_2), \\
u_z^- (L_2) = 0 & r \in (0, R_2), \\
u_z^+ (L_1) = u_z^- (L_1) & r \in (R_1, R_2), \\
u_z^+ (0) = 0 & r \in (R_1, R_2),
\end{cases}
$$

and the equilibrium $\pi\sigma_{zz}^+ \left(R_2^2 - R_1^2\right) - \pi\bar{p}R_1^2 = \pi\sigma_{zz}^- R_2^2$ at $z = L_1$ are satisfied. By neglecting the terms of higher order then ϵ^2, we obtain

$$
C_1^+ = \frac{-2p\epsilon^2}{E_m} \left(1 + v_m\right),
$$

$$
C_2^+ = \frac{R_1^2(1+v_m)}{E_m} \left\{ \bar{p}\frac{-\epsilon^2 v_m(1-\chi)}{v_m} \right.
$$
$$
\left. + p \left[1 + \frac{\epsilon^2}{1-2v_m}\left(-1 + \frac{2v_m^2(1-\chi)}{1-2v_m}\right)\right]\right\},
$$

$$
C_3^- = \frac{\epsilon^2 \chi}{E_m(1-v_m)} \left(\bar{p} + p\frac{2v_m}{1-2v_m}\right), \qquad C_1^- = 0, \qquad C_4^- = 0,
$$

where $\chi = L_1/L_2$, $\epsilon = R_1/R_2$, v_m, E_m are the Poisson ratio and Young modulus of the elastic medium, respectively. In a similar way, in the case of the elastic cylinder, the solution of Eq. (2) is given by $u_r(r) = C_1 r/2$ and $u_z(z) = C_3 z$ with $(r, z) \in C$. By imposing the following boundary conditions

$$
\begin{cases}
\sigma_{rr} = -p & r = R, \quad z \in (0, L), \\
\sigma_{zz} = -\bar{p} & z = L, \quad r \in (0, R), \\
u(0) = 0 & r \in (0, R),
\end{cases}
$$

the solution, in the case of the elastic cylinder, is given by $C_1 = [-p\left(1 - v_c\right) + v_c\bar{p}]/E_c$ and $C_3 = (2v_c p - \bar{p})/E_c$, where v_c, E_c correspond to the elastic cylinder coefficients. In order to have the contact at the interface between the matrix and the elastic cylinder, we require the following compatibility equation

$$
\begin{cases}
R + u_r(R) = R_1 + u_r^+(R_1), \\
L + u_z(L) = L_1 + u_z^+ (L_1),
\end{cases}
$$

the radius and length of the deformed elastic root are equal to the radius and length of the deformed matrix, respectively. By exploiting the compatibility conditions at the contact and after some algebra, we obtain the expressions for axial, $\bar{p}$, and radial pressure, p, in a

dimensional form

$$
\bar{p} = E_c \frac{\left(1 - v_c\right)\left(R + R_1 A_2\right)\left(L - L_1\right) + 2v_c(L - L_1 A_1)(R - R_1)}{\left(1 - v_c\right)\left(R + R_1 A_2\right)\left(L + L_1 B_1\right) - 2v_c^2(L - L_1 A_1)(R - R_1 A_1)},
\tag{3.1}
$$

$$
p = E_c \frac{v_c\left(R - R_1 A_1\right)\left(L - L_1\right) + (L - L_1 B_1)(R - R_1)}{\left(1 - v_c\right)\left(R + R_1 A_2\right)\left(L + L_1 B_1\right) - 2v_c^2(L - L_1 A_1)(R - R_1 A_1)},
\tag{3.2}
$$

where

- $A_1 = \epsilon^2 \frac{E_c}{E_m} v_m \frac{(1-\chi)(1+v_m)}{v_c(1-v_m)}$,
- $A_2 = \frac{E_c}{E_m} \frac{(1+v_m)}{(1-v_c)}\left[1 - \epsilon^2 + \frac{\epsilon^2}{1-2v_m}\left(\frac{2v_m^2(1-\chi)}{1-v_m} - 1\right)\right]$,
- $B_1 = \epsilon^2 \frac{E_c}{E_m}(1 - \chi)(1 + v_m)$
- $\epsilon = R_1/R_2$, $\chi = L_1/L_2$.

3. Theoretical translation of biological phenomena

We present a mathematical model describing the effect of mechanical stresses on plant root growth. The model shows how the axial stress at the contact affects the plant root growth in the surrounding environment. When the soil is hard to penetrate, an individual root may stop growing [9]. Therefore, we use a Fracture–Regrowth Cycle, FRC, as in [33] by including also the condition that the root stops its growth when a threshold axial pressure is reached. If $\bar{p}_{fr}$ is the fracture stress of the surrounding elastic medium and $\bar{p}_c$ is the maximum pressure that a root can exert to grow, two cases can occur:

(a) $\bar{p}_{fr} \geq \bar{p}_c$. The elastic root can grow until the axial stress $\bar{p}$ reaches the critical value and there is no fracture of the elastic matrix, i.e. the root stops growing when $\bar{p} = \bar{p}_c$. It may be the limit case of a root growing in very strong soils.

(b) $\bar{p}_{fr} < \bar{p}_c$. The axial stress $\bar{p}$ can reach the fracture stress $\bar{p}_{fr}$ and a new growth cycle begins. In particular, each cycle starts with the initial length equal to the growing zone length and ends when the axial stress, $\bar{p}$, at the contact reaches soil failure, $\bar{p}_{fr}$. Therefore, the root relaxes, the increase in root length is stored, and a new cycle starts with the updated root length.

We focus on the case (b) and Algorithm 1 shows a brief outline of the solution algorithm implementing the FRC. In the following Subsections, we introduce the growth equations coupled with Eq. (3.1) to compare our theoretical results with the experiments in artificial soils (see Appendix A for details). In particular, the artificial soils were prepared with different Phytagel concentrations (PC) and different nutrient concentrations were obtained using Murashige and Skoog Basal Salt Mixture (MS). In the first case, we compare the theoretical results with data collected in different Phytagel concentrations, while in the second case with an excessive nutrient concentration in the artificial soil medium. In addition, for the first case, we compare our theoretical results with data from experiments in different real soil compactions (for more details see [9]).

In this work, the main assumptions related to the growth process are the following:

- The root is cylindrical and is a linearly elastic, homogenous, and isotropic material;
- The surrounding matrix is a linearly elastic, homogenous, and isotropic fracturable material;
- The growth is related to a single isolated root in the axial direction;
- The growth is uniformly distributed at the root apical zone due to cell division and extension;
- The growing zone has the same length and number of cells at the beginning of each FRC;
- The pressure is zero at both ends of each FRC.

---

[1] All the derivatives with respect to θ vanish and there is no dependence of the angle θ.

Algorithm 1: Solution algorithm for the axial growth case implementing the FRC ($\bar{p}_{fr} < \bar{p}_c$).

$t_{fr}^0 = 0$
while $t_{fr}^{i-1} \neq t_{end}$
  1. Solve growth equation using the expression of the axial pressure, $\bar{p}$, obtained by the inclusion problem.
  2. Take and store the solution (t, L) that satisfies $\bar{p} \leq \bar{p}_{fr}$.
  3. Compute and store the relaxed length at the end of the i-FRC.
  4. Update the total length at the end of the i-FRC.
  5. Update time and length to set the initial condition for the $(i+1)$-FRC : $t_0^{i+1} = t_{fr}^i$, $L(t_0^{i+1}) = L(t_0)$.
  $i := i + 1$
end

3.1. Case I: axial expansion

3.1.1. Growth equation

By exploiting a similar approach to Lockhart [20] and by taking into account the soil impedance as in [21,39–41], we can describe the growth process with the following model[2]

$$\frac{1}{V} \cdot \frac{dV}{dt} = \Phi \left(\bar{p} - \bar{p}_c \right)_+ , \tag{4}$$

where V is the volume of the root growing zone, Φ, $[\Phi] = (\text{MPa} \cdot \text{s})^{-1}$, is related to the extensibility of wall of a plant cell and $\bar{p}_c$ is the threshold value introduced at the beginning of this Section. The model (4) captures the most commonly accepted phenomenon related to the influence of soil physical properties on root growth, i.e. roots grow slower in denser soils. In order to consider not only the influence of the soil impedance on the root growth but also the input power from the surrounding matrix, the energy rate of consumption due to the metabolism and growth, we adopt the growth model reported in [33] but considering the axial pressure as confining pressure

$$\eta \frac{dN}{dt} + \bar{p} \frac{dV}{dt} + \beta N = \gamma N^\rho , \tag{5}$$

where

- $N = M/m = V/v$ represents the total number of cells in the growing zone of the plant root; and $M(V)$, $m(v)$ are the mass (volume) of the root growing zone and average mass (volume) of a single cell, respectively;
- η is the energy required to create a new cell;
- β is the metabolic rate for a single cell;
- $\gamma N^\rho = \alpha (m)^\rho N^\rho = \alpha M^\rho$ is the input power from the surrounding matrix and $\rho = 3/4$. Since we focus on the growth of the primary root, we assume that the plant seed continuously supplies nutrients and the surrounding matrix is only an external source of water. In the case of older plant roots, we can consider the matrix is a continuously-replenished medium.
- $\bar{p}$ is the axial pressure experienced by the growing root tip at the boundary between root and matrix.

For simplicity, we consider a uniformly distributed growth at the apical zone through cell division and cell extension. Clearly, since we pursue an approach based on the mechanical interaction between the root and the soil, we disregard to model the water flow in both the root system and the surrounding soil. The Eq. (5) is of the growth equation proposed in [33]. This approach has been applied to a wide range of biological phenomena [42,43]. For example, the authors of [33] developed a model for tumor invasion, considering the effect of interfacial pressure as an extension of the West, Brown, and Enquist law [44]. The root elongation rate is sensitive to variations in axial pressure [45,46], but insensitive to radial pressure [47]. This aspect explains the presence of the mechanical term in Eqs. (4) and (5) due to the axial pressure. We

---

[2] $(f(x))_+ = \max(f(x), 0)$.

---

will further assume that the root is cylindrical (as in Fig. 2) and grows only in length. Therefore, an increase in length is related to an increase in volume and in the number of cells through

$$\frac{dL}{dt} = \frac{1}{\pi R^2} \frac{dV}{dt} = \frac{v_0}{\pi R^2} \frac{dN}{dt} ,$$

where v_0 is the single cell volume that we consider constant. Note that if $\rho = 1$ and if $\bar{p}$ is small, with proper values of v_0, η, γ, β we can recover the Eq. (4) from the Eq. (5).

3.1.2. Dimensionless formulation

We recast the growth problem in a dimensionless form. We introduce the dimensionless quantities $L^* = L/L_0$, $t^* = t/t_{ref}$, where L_0 represents the length of the growing region and t_{ref} is the duration of the experiment. We assume $L_0 = 3$ mm and $t_{ref} = 3$ days.

Remark 1. L_1^* represents the initial length of the elastic cylinder in each cycle and we assume zero pressure at both ends of the cycle. Therefore, we can write $L_1 = L_0 L^*(t_0)$, where the adimensional length $L^*(t_0)$ is "updated" at the beginning of each cycle.

Omitting the "*", in the case of axial growth, i.e. $R = R_1$, we can rewrite Eqs. (3.1) and (3.2) as

$$\begin{cases} \bar{p} = \Theta_1 \dfrac{L - \Theta_2}{L + \Theta_3} , \\ p = \Theta_4 \dfrac{L - \Theta_2}{L + \Theta_3} , \end{cases} \tag{6}$$

where

- $\Theta_1 = E_c \frac{\Lambda_1}{\Lambda_2}$,
- $\Theta_2 = L(t_0)$ is the root length at the beginning of the FRC;
- $\Theta_3 = \frac{\Lambda_3}{\Lambda_2} \epsilon^2 \frac{E_c}{E_m} L(t_0)(1 - \chi)(1 + v_m)$,
- $\Theta_4 = \frac{E_c}{\Lambda_2} \left[v_c - \epsilon^2 \frac{E_c}{E_m} (1 - \chi) \frac{v_m(1+v_m)}{(1-v_m)} \right]$,
- $\Lambda_1 = 1 - v_c + \frac{E_c}{E_m}(1 + v_m) \left[1 - \epsilon^2 + \frac{\epsilon^2}{1-2v_m} \left(\frac{2v_m^2(1-\chi)}{1-v_m} - 1 \right) \right]$,
- $\Lambda_2 = \Lambda_1 + \frac{E_c}{E_m} (1 + v_m) \frac{2v_m v_c \epsilon^2 (1-\chi)}{(1-v_m)^2} - 2v_c^2$,
- $\Lambda_3 = \Lambda_1 - \frac{E_c}{E_m} (1 + v_m) \frac{2v_m^2 \epsilon^2 (1-\chi)}{(1-v_m)^2} - \frac{2v_m v_c}{1-v_m}$,

and $[\Theta_1] = [\Theta_4] = \text{MPa}$ and $[\Theta_2] = [\Theta_3] = 1$.

By considering the stop of the root growth when $\bar{p}$ reaches the critical value $\bar{p}_c$, from Eq. (5) we have $\beta = \gamma \left(\frac{\Theta_2 + \Theta_3 \bar{p}_c/\Theta_1}{1 - \bar{p}_c/\Theta_1} \right)^{\rho-1}$ and we introduce the scaling parameter Θ_1 for the adimesionalization of the axial pressure, $\bar{p}$, as an upper bound for $\bar{p}_c$.

In addition, we analyze how the axial stress at the contact can affect the biomechanical properties of plant root penetration depending on the surrounding matrix. Since the change in length is slow, every moment of the growth process can be represented as a static state and we can interpret the mechanical process of root growth as an
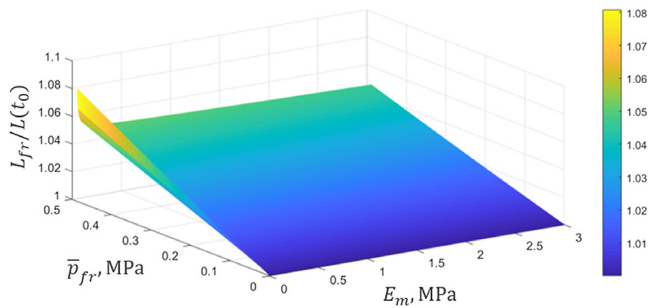
Fig. 3. Plot of the ratio between the root length at $\bar{p} = \bar{p}_{fr}$ and the root initial length in adimensional form, $L_{fr}/L(t_0)$, considering the critical growth pressure as $\bar{p}_c = 0.5$ MPa, the root Young modulus as $E_c = 10$ MPa, the Poisson ratio for both root and soil as $v_m = v_c = 0.49$, the root and hole radius as $R = R_1 = 0.588$ mm, and the outer radius of the soil as $R_2 = 30$ mm.

inclusion model. The inclusion model analyzes in detail the mechanical expansion of an elastic cylinder in a cylindrical hole of an elastic fracturable medium. In particular, we study the sensitivity of the root length to the variation in the fracture stress, $\bar{p}_{fr}$, and the Young modulus, E_m, of the surrounding matrix. Therefore, we analyze the variation in the root length, L_{fr}, when the axial contact pressure is equal to $\bar{p}_{fr}$. From Eq. (6), we can obtain the expression of root length in the dimensionless form at $\bar{p} = \bar{p}_{fr}$

$$L_{fr} = \frac{L(t_0) + \Theta_3 \frac{\bar{p}_{fr}}{\Theta_1}}{1 - \frac{\bar{p}_{fr}}{\Theta_1}}, \qquad \forall \bar{p}_{fr} < \Theta_1. \tag{7}$$

Since $L_1 \ll L_2$, we consider $\chi = L_1/L_2 \to 0$, but we maintain the order of approximation of $\epsilon = R_1/R_2$.

We consider $L_{fr} = L_{fr}(\bar{p}_{fr}, E_m)$, i.e. as a function of both failure stress, $\bar{p}_{fr}$, and the elastic modulus of the surrounding medium, E_m. The plot of $L_{fr}(\bar{p}_{fr}, E_m)$ is shown in Fig. 3, which highlights that when

1. $\bar{p}_{fr} = k \cdot E_m$, L_{fr} is an increasing function of E_m for values of E_m enough small such that $L_{fr} > 0$ and $\bar{p}_{fr} < \bar{p}_c$;
2. $E_m = constant$, L_{fr} is an increasing function of $\bar{p}_{fr}$ such that $L_{fr} > 0$ and $\bar{p}_{fr} < \bar{p}_c$;
3. $\bar{p}_{fr} = constant < \bar{p}_c$, L_{fr} is a decreasing function of E_m such that $L_{fr} > 0$.

The above analysis highlights the importance of considering the concept of failure stress at a small value for Young's modulus of the elastic matrix.

3.2. Case II: axial and radial expansion

3.2.1. Growth equations
We couple equation (5) with the following

$$\frac{dR}{dt} \cdot \frac{1}{R} = \left(1 - \frac{\gamma_{Cc}}{\gamma}\right)_+ \cdot \frac{dN}{dt} \cdot \frac{1}{N}. \tag{8}$$

Now, Eqs. (5) and (8) include both axial and radial growth. In particular, the axial pressure, $\bar{p}$, at the boundary between the root tip and matrix depends on both root length and radius (see Section 2). In Eq. (8), we take into account the estimated value, γ_{Cc}, of the previous case, i.e. without nutrient in the soil, meaning that the plant seed furnishes nutrients and the surrounding medium supplies continuously only water (γ_{Cc} corresponds to the parameter γ of the previous case, Section 3.1.1). In order to include the effect of the nutrient in the soil, Eq. (8) considers that the radial swelling occurs only when the scaling parameter γ of the input power from the surrounding soil is higher than γ_{Cc} (Fig. 4). By assuming that the root is cylindrical, the increase in length, L, is given by $\frac{dL}{dt} = \frac{v_o}{\pi R^2} \left(\frac{dN}{dt} - \frac{2N}{R} \cdot \frac{dR}{dt}\right)$. We

consider that the total number of cells in a plant root is $N = V/v_0$, where V is the root volume of the growing zone and v_0 is the average of a single cell volume. We update v_0 with the non-dimensional initial root radius at each FRC to indicate the possible thickening of cells due to the chemical stimulus.

3.2.2. Dimensionless formulation
We scale the variables L and t as in Section 3.1.2. In addition, we scale $R = R_0 R^*$ where R_0 the values of the top diameter at the third day of life (see Appendix A).

Remark 2. L_1, R_1 represent the initial length and radius of the elastic cylinder, respectively, in each cycle and we assume zero pressure at both ends of the cycle. Therefore, we can write $L_1 = L_0 L^*(t_0)$, $R_1 = R_0 R^*(t_0)$, where the dimensionless length $L^*(t_0)$ and radius $R^*(t_0)$ are "updated" at the beginning of each cycle. By assuming the same length growing zone and number of cells at the beginning of each FRC with an increasing radius ($v_0 N(t_0) = \pi L(t_0) R^2(t_0)$), we update the single cell volume v_0 with the non-dimensional initial root radius in each FRC, i.e. $v_0 \propto R^{*2}(t_0)$.

By omitting the "*" and assuming that the root growth ends when $\bar{p} = \bar{p}_c$, from Eq. (5), now, we obtain $\beta = \gamma N_c^{\rho-1}$, $\rho = 3/4$,

$$N_c = N(t_0) \frac{1 + \frac{\bar{p}_c}{E_c}\left(\frac{U_1 B_1 - U_2 A_1}{U_1}\right)}{1 - \frac{\bar{p}_c}{E_c}\left(\frac{U_1 - U_2}{U_1}\right)}, \tag{9}$$

where

- $U_1 = (1 - v_c)(1 + A_2)$,
- $U_2 = 2v_c^2(1 - A_1)$,
- $A_1 = \epsilon^2 \frac{E_c}{E_m} v_m \frac{(1-\chi)(1+v_m)}{v_c(1-v_m)}$,
- $A_2 = \frac{E_c}{E_m} \frac{(1+v_m)}{(1-v_c)} \left[1 - \epsilon^2 + \frac{\epsilon^2}{1-2v_m}\left(\frac{2v_m^2(1-\chi)}{1-v_m} - 1\right)\right]$.

In the case of axial growth, Eq. (9) corresponds to Eq. (7).

4. Results and discussion

4.1. Case I: axial expansion

In this analysis, the surrounding medium is assumed to be an infinite body with respect to the plant root, so that $R, R_1 \ll R_2$ and $L, L_1 \ll L_2$. Therefore, to obtain the numerical solutions, we set $\chi = L_1/L_2 = 0$, and we assume $R_2 = 30$ mm for both artificial and real soils. We then assume that the critical growth pressure $\bar{p}_c = 0.5$ MPa (for the value range of $\bar{p}_c$ see, e.g., [9,17–19]), and the root Young modulus $E_c = 10$ MPa [48]. We assume that $R_1 = R$ are equal to the values of the root apex radius at the third day of life (see Appendix A) for artificial soil, and $R_1 = R = 0.6$ mm for real soils. Both Poisson's ratios are $v_{m,c} = 0.49$ for Phytagel and $v_c = 0.49, v_m = 0.45$ for soils [49–51]. The values used for γ, E_m, $\bar{p}_{fr}$ are reported in Table 1 (E_m, $\bar{p}_{fr}$ are obtained by means of compression tests, Appendix A). In order to estimate only the variation of γ with respect the different soil media, a constant value for the parameter η, $\eta = 1$ MPa·mm^3, has been chosen. Figs. 5 and 6 show the evolution of the root length with time for artificial and real soils, respectively. In order to assess the influence of γ on the variation of the final root length, we carry out the theoretical predictions in both artificial and real soil using all the combinations of the value for γ listed in Table 1. The results by means of Eq. (5) are given in Fig. 7a, b. The value of the scaling parameter γ of the energy released from the seed increases with both the Phytagel concentration and the real soil compaction (Table 1). By using artificial growth media, roots, which were grown in harder soils, were longer than the roots grown in softer soils, while in real soils this was not the case, see Figs. 5–7b. In the only case of 0.6% Phytagel we obtain a lower final length in both the numerical (Fig. 7b) and experimental results (see Appendix A).
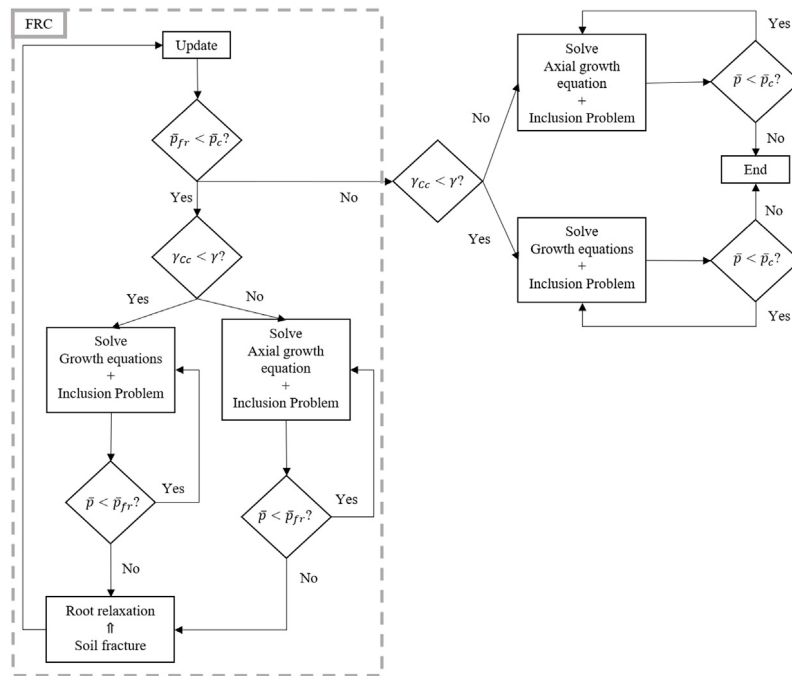
Fig. 4. Schematic diagram of the root control mechanism to nutrient stress. The initial conditions are differently updated if the root activates the radial swelling as a response to nutrient stress ($\gamma_{Cc} < \gamma$). In such a case, the initial root length, diameter, and cell volume are updated and stored, otherwise, only the root initial length is stored. Each cycle starts with updated initial conditions and ends when the soil medium fractures, i.e. the axial stress, $\bar{p}$, at the contact equals the soil failure, $\bar{p}_{fr}$. Therefore, the root relaxes and a new cycle starts with the updated initial conditions. Otherwise, the fracture in the matrix does not occur and the root grows until the growth critical pressure, $\bar{p}_c$.

Phytagel is a hard and brittle homogeneous gel [52] and, because of its homogeneity, we can assume that the increase in Young modulus leads to an increase in the fracture stress (see Section 3.1.2). In addition, Fig. 7c shows that γ increases linearly with respect to the Phytagel concentration. Therefore, in the presence of artificial soils, the increase in energy availability and the soil mechanical properties may enhance root penetration.

4.2. Case II: axial and radial expansion

The theoretical results are performed by means of the Eqs. (5) and (8) applied to the growing zone of the root and the related surrounding medium (Fig. 2). We suppose that the soil is greater than the root, i.e. $R, R_1 \ll R_2$ and $L, L_1 \ll L_2$ and we set the values of the parameters χ, R_2, $\bar{p}_c$, $E_{m,c}$, $v_{m,c}$, $\bar{p}_{fr}$ and η as in Section 4.1. The estimated values of γ for *Zea mays* roots grown in artificial soil without nutrients are in Table 1 and we refer to those values as γ_{Cc} in this Subsection. Since the experimental data show an abnormal radial expansion only in the case of the highest concentration of nutrients (MS4, see Appendix A) at 0.3, 0.6, and 0.9% Phytagel concentration, we compare the numerical solution with the latter set of data. Since we have observed that the radial swelling of 17% at the height of the meristematic area occurs in the 5–6-day old roots for the MS4 concentration with respect to the mature region, we consider the increase of 17% in the top diameter at the 6-day age for the comparison with the numerical solutions (see Appendix A). The estimated value of the parameter γ related to the nutrient availability in the case of nutrients in the artificial soil at 0.3, 0.6, and 0.9% Phytagel concentration are $9.054 \cdot 10^{-5}$, $1.157 \cdot 10^{-4}$, and $1.839 \cdot 10^{-4}$ MPa $\cdot$ mm³/s. The value of the scaling parameter γ of the input power from the surrounding matrix increases with both the Phytagel concentration and the MS concentration. The results from the Eqs. (5) and (8) are given in Fig. 8. The numerical result of the MS4 at 0.3% Phytagel concentration is smaller than the measured data for the same elongation reduction. Moreover, we obtain a good agreement with the evolution of the root length, while the root radius is underestimated with respect to the experimental data. It is worth noting

that Eq. (8) cannot allow a decrease in root radius, since γ_{Cc} represents the parameter related to the energy released by seed without nutrients in soil and the soil medium is only an external source of water.

The biological mechanism observed in our experiments (Appendix A) could be similar to salt toxicity as observed in [8]. In addition, other studies show similar root apex swellings, e.g. after depletion of gibberellic acid or ethylene and high calcium exposures [15,16,53]. In addition, investigations on the depolymerization of F-actin with latrunculin B reveal also in very similar maize root apex swellings and inhibition of the root cell elongation [13]. Therefore, a possible adaptive strategy to nutrient stress could be the enlargement of cells (as supposed in Section 3.2.2), inducing a swelling of root apex (see Appendix A). This strategy should help cells to uptake more water and create a stronger barrier to reduce toxic nutrient concentration [8].

5. Conclusions

The aim of this work is to present a mathematical model for the growth of plant roots in a soil medium. In particular, we developed a theoretical framework and an *ad-hoc* setup for better understanding the contribution that mechanical stimuli play in the root growth in the case of *Z. mays* primary root. Our theoretical and experimental studies may be a further investigation to explain how plant roots could control the growth in response to the contact with the surrounding medium. We obtained different mechanical responses of the root growth depending on different mechanical properties of its environment in agreement with the experimental investigations (1) with different artificial soil concentration and real soil compactness in absence of nutrients and (2) with different nutrient concentrations in artificial soil. In all the cases, the scaling parameter γ related to the input energy increases with the artificial soil concentration and real soil compactness. In addition, for artificial soils with high nutrient concentration we obtained the reduction in root elongation as in experimental data but with an underestimated radial expansion.

The mathematical model is based on continuum mechanics and is a general formulation for any type of inclusion problem in the

Table 1
Values of parameters used in the numerical solutions for the growth model. PC is the Phytagel concentration.

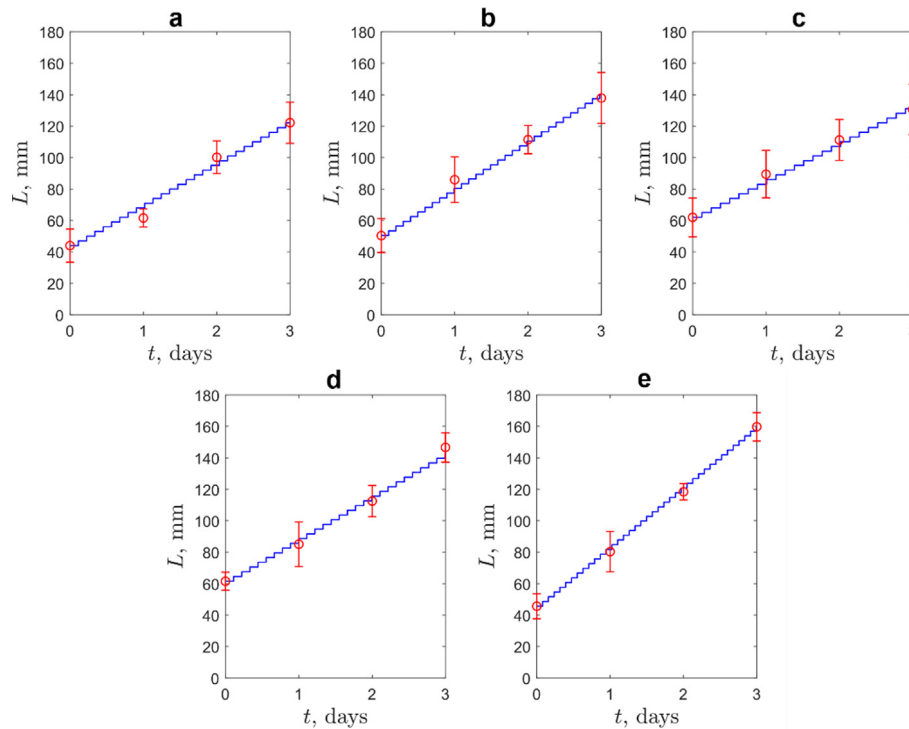|		E_m (MPa)	$\bar{p}_{fr}\pm$ SD (MPa)	γ (MPa mm^3/s)
Phytagel	0.15% PC	$1.02 \cdot 10^{-2}$	$0.0025 \pm 7.2775 \cdot 10^{-4}$	$2.17 \cdot 10^{-5}$
	0.3% PC	$1.82 \cdot 10^{-2}$	0.0053 ± 0.0012	$5.56 \cdot 10^{-5}$
	0.6% PC	$4.23 \cdot 10^{-2}$	0.0089 ± 0.0016	$7.26 \cdot 10^{-5}$
	0.9% PC	$7.43 \cdot 10^{-2}$	0.0140 ± 0.0018	$1.31 \cdot 10^{-4}$
	1.2% PC	$8.09 \cdot 10^{-2}$	0.0141 ± 0.0017	$1.89 \cdot 10^{-4}$
Real soil [9]	Low compaction	2	0.02	$3.37 \cdot 10^{-4}$
	Medium compaction	25	0.04	$6.3 \cdot 10^{-4}$
	High compaction	50	0.25	0.0029

Fig. 5. Comparison of the empirical data (red circles) in artificial soils (mean values ±SD) and analytical solution (blue line) at (a) 0.15, (b) 0.3, (c) 0.6, (d) 0.9, and (e) 1.2% Phytagel concentration. Each step of the analytical solution represents a cycle, which ends with the fracture of the soil and begins after the relaxation of the root.

Fig. 6. Comparison of the empirical data (red circles) in real soils and analytical solution (blue lines) at (a) low, (b) medium, and (c) high soil compaction. Each step of the analytical solution represents a cycle, which ends with the fracture of the soil and begins after the relaxation of the root.
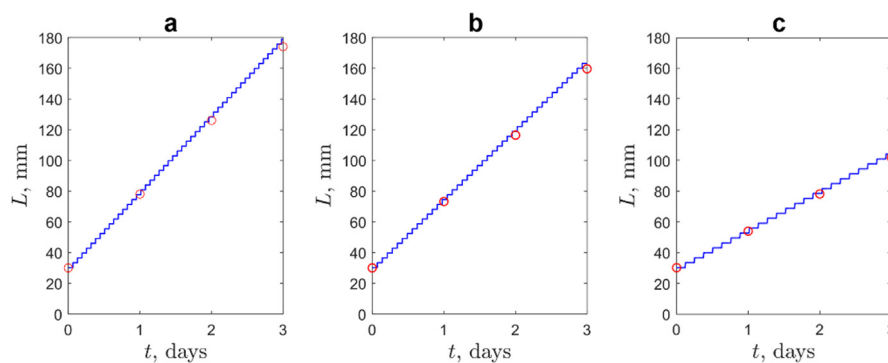
context of linear elasticity. This study may help to improve the current knowledge of the behavioral strategies of plant roots as a starting point for constructing more complete predictive models, e.g. related to the mechanical properties of both the root tissues and the soil medium, the hydraulics of root growth, an explicit distinction in the growth process of cell division and cell elongation, and the assumption of a cylindrical root. Thus, a multidisciplinary approach with the synergy of modeling, engineering and plant science will be required towards a better understanding of the mechanical behavior of complex biological systems.

Declaration of competing interest

The authors declare that they have no known competing financial interests or personal relationships that could have appeared to influence the work reported in this paper.
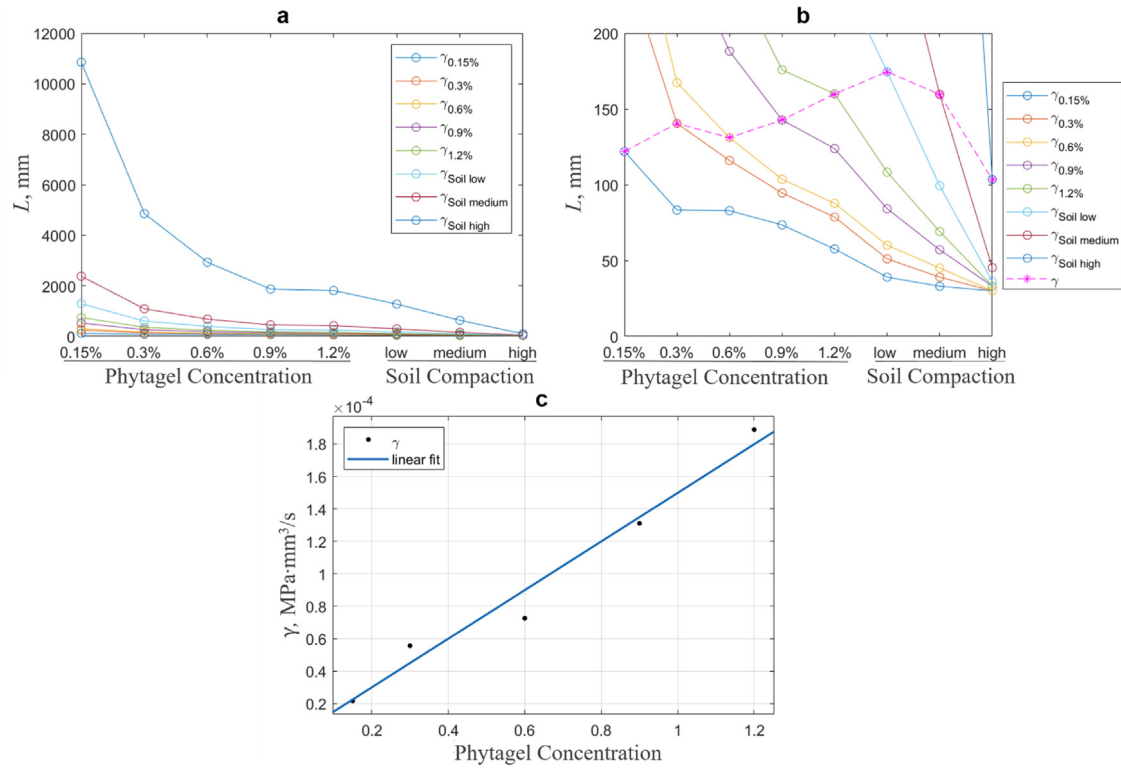
Fig. 7. (a) In each soil medium we evaluated the variation of the root length at the sixth day of life, by considering all the combinations of the values for the scaling parameter γ of the input power from the plant seed, exploited in the numerical solution (Table 1); (b) The dotted line represents the variation of the root length in the numerical solutions of Figs. 5 and 6; (c) The linear fit of γ and different concentrations of Phytagel (R-squared: 0.97; $y = a \cdot x$, $a = 1.498 \cdot 10^{-2}$ MPa mm^3/s).
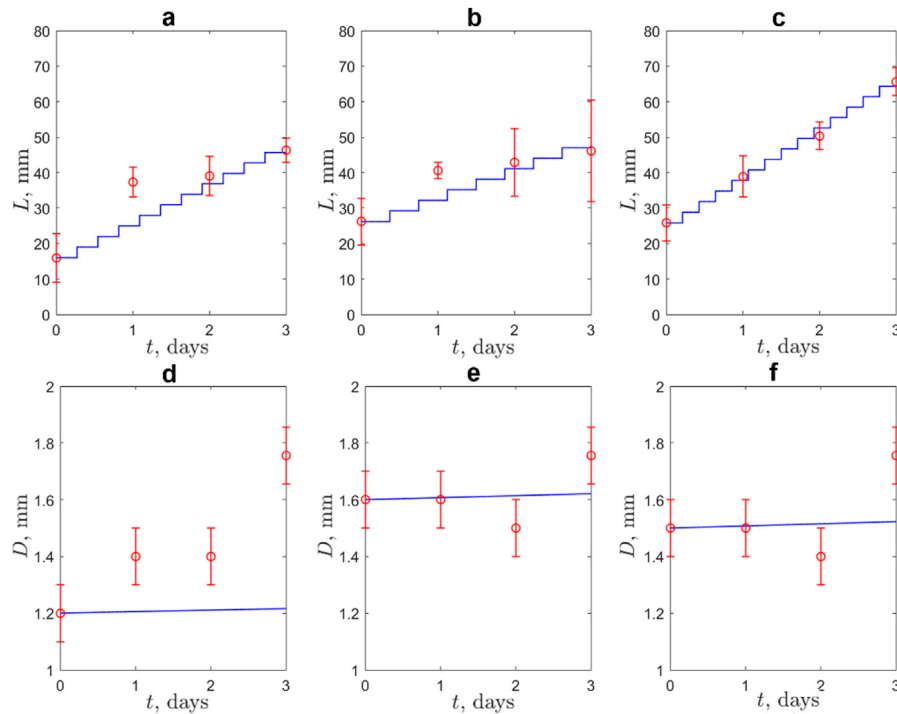

Fig. 8. Numerical solution of (a)–(c) the length and (d)–(f) the radius evolution against time (blue line). The red circles are the empirical data (mean values ±SD) in the case of MS4 concentration at (a), (d) 0.3, (b), (e) 0.6, and (c), (f) 0.9% Phytagel concentration.

Acknowledgments

Appendix A. Supplementary data

Supplementary material related to this article can be found online at https://doi.org/10.1016/j.ijnonlinmec.2019.103344.

References

[1] D. Foehse, A. Jungk, Influence of phosphate and nitrate supply on root hair formation of rape, spinach and tomato plants, Plant Soil 74 (1983) 359–368, http://dx.doi.org/10.1007/BF02181353.

[2] L. Sánchez-Calderón, M.E. Ibarra-Cortés, I. Zepeda-Jazo, Root development and abiotic stress adaptation, in: Agric. Biol. Sci. Abiotic Stress - Plant Responses Appl. Agric., 2013, http://dx.doi.org/10.5772/55043.

[3] A.D. Bradshaw, Evolutionary significance of phenotypic plasticity in plants, Adv. Genet. 13 (1965) 115–155, http://dx.doi.org/10.1016/S0065-2660(08)60048-6.

[4] J.P. Grime, J.M.L. Mackey, The role of plasticity in resource capture by plants, Evol. Ecol. 16 (2002) 299–307, http://dx.doi.org/10.1023/A:1019640813676.

[5] S. Filleur, P. Walch-Liu, Y. Gan, B.G. Forde, Nitrate and glutamate sensing by plant roots, Biochem. Soc. Trans. 33 (2005) 283–286, http://dx.doi.org/10.1042/BST0330283.

[6] K.P. Barley, Influence of soil strength of growth of roots, Soil Sci. 96 (1963) 175–180, http://dx.doi.org/10.1097/00010694-196309000-00004.

[7] A.G. Bengough, C.E. Mullins, Mechanical impedance to root growth: a review of experimental techniques and root growth responses, J. Soil Sci. 41 (1990) 341–358, http://dx.doi.org/10.1111/j.1365-2389.1990.tb00070.x.

[8] H. Li, S. Yan, L. Zhao, J. Tan, Q. Zhang, F. Gao, P. Wang, H. Hou, L. Li, Histone acetylation associated up-regulation of the cell wall related genes is involved in salt stress induced maize root swelling, BMC Plant Biol. 14 (2014) http://dx.doi.org/10.1186/1471-2229-14-105.

[9] L. Popova, D. van Dusschoten, K.A. Nagel, F. Fiorani, B. Mazzolai, Plant root tortuosity: an indicator of root path formation in soil with different composition and density, Ann. Bot. 118 (2016) 685–698, http://dx.doi.org/10.1093/aob/mcw057.

[10] B. Atwell, Physiological responses of lupin roots to soil compaction, in: B.C. Loughamn, O. Gašparíková, J. Kolek (Eds.), Struct. Funct. Asp. Transp. Roots Third Int. Symp. 'Structure Funct. Roots' Nitra, Czechoslov. 3–7 August 1987, Kluwer Academic Publishers, 1989, pp. 251–255.

[11] A.J. Wilson, A.W. Robards, M.J. Goss, Effects of mechanical impedance on root growth in barley, Hordeum vulgare L.: II. Effects on cell development in seminal roots, J. Exp. Bot. 28 (1977) 1216–1227, http://dx.doi.org/10.1093/jxb/28.5.1216.

[12] F. Baluška, E. Busti, S. Dolfini, G. Gavazzi, D. Volkmann, Lilliputian mutant of maize lacks cell elongation and shows defects in organization of actin cytoskeleton, Dev. Biol. 236 (2001) 478–491, http://dx.doi.org/10.1006/dbio.2001.0333.

[13] F. Baluška, J. Jasik, H.G. Edelmann, T. Salajová, D. Volkmann, Latrunculin B-induced plant dwarfism: Plant cell elongation is F-actin-dependent, Dev. Biol. (2001) http://dx.doi.org/10.1006/dbio.2000.0115.

[14] F. Baluska, J.S. Parker, P.W. Barlow, A role for gibberellic-acid in orienting microtubules and regulating cell-growth polarity in the maize root cortex, Planta 191 (1993) 149–157.

[15] F. Baluška, J.S. Parker, P.W. Barlow, The microtubular cytoskeleton in cells of cold-treated roots of maize (Zea mays L.) shows tissue-specific responses, Protoplasma 172 (1993) 84–96, http://dx.doi.org/10.1007/BF01379366.

[16] F. Baluska, R.W.I. Brailsford, M. Hauskrecht, M.B.I. Jackson, P.W. Barlow, Cellular dimorphism in the maize root cortex : Involvement of microtubules, in: Ethylene and Gibberellin in the Differentiation of Cellular Behaviour in Postmitotic Growth Zones, 1993, pp. 394–403.

[17] R.K. Misra, A.R. Dexter, A.M. Alston, Maximum axial and radial growth pressures of plant roots, Plant Soil 95 (1986) 315–326, http://dx.doi.org/10.1007/BF02374612.

[18] A.G. Bengough, B.M. McKenzie, P.D. Hallett, T.A. Valentine, Root elongation, water stress, and mechanical impedance: A review of limiting stresses and beneficial root tip traits, J. Exp. Bot. 62 (2011) 59–68, http://dx.doi.org/10.1093/jxb/erq350.

[19] L.J. Clark, W.R. Whalley, P.B. Barraclough, How do roots penetrate strong soil?, Plant Soil (2003) 93–104, http://dx.doi.org/10.1023/A:1026140122848.

[20] J.A. Lockhart, An analysis of irreversible plant cell elongation, J. Theoret. Biol. 8 (1965) 264–275, http://dx.doi.org/10.1016/0022-5193(65)90077-9.

[21] E.L. Greacen, J.S. Oh, Physics of root growth, Nat. New Biol. 235 (1972) 24–25, http://dx.doi.org/10.1038/newbio235024a0.

[22] D. Cosgrove, Wall extensibility: its nature, measurement and relationship to plant cell growth, New Phytol. 124 (1992) 1–23.

[23] J. Pritchard, The control of cell expansion in roots, New Phytol. 127 (1994) 3–26.

[24] S. Lewicka, M. Pietruszka, Anisotropic plant cell elongation due to ortho-gravitropism, J. Math. Biol. (2007) 91–100, http://dx.doi.org/10.1007/s00285-006-0049-3.

[25] J.C. Crick, J.P. Grime, Morphological plasticity and mineral nutrient capture in two herbaceous species of contrasted ecology, New Phytol. 107 (1987) 403–414, http://dx.doi.org/10.1111/j.1469-8137.1987.tb00192.x.

[26] M.C. Drew, L.R. Saker, Nutrient supply and the growth of the seminal root system in barley: III. Compensatory increases in growth of lateral roots, and in rates of phosphate uptake, in response to a localized supply of phosphate, J. Exp. Bot. 29 (1978) 435–451, http://dx.doi.org/10.1093/jxb/29.2.435.

[27] K.L. Gross, A. Peters, K.S. Pregitzer, Fine root growth and demographic responses to nutrient patches in four old-field plant species, Oecologia 95 (1993) 61–64, http://dx.doi.org/10.1007/BF00649507.

[28] R.B. Jackson, M.M. Caldwell, The timing and degree of root proliferation in fertile-soil microsites for three cold-desert perennials, Oecologia 81 (1989) 149–153, http://dx.doi.org/10.1007/BF00379798.

[29] R.B. Jackson, M.M. Caldwell, Integrating resource heterogeneity and plant plasticity: Modelling nitrate and phosphate uptake in a patchy soil environment, J. Ecol. 84 (1996) 891, http://dx.doi.org/10.2307/2960560.

[30] J. Kirby, A. Bengough, Influence of soil strength on root growth : experiments and analysis using a critical-state model, Eur. J. Soil Sci. 53 (2002) 119–128, http://dx.doi.org/10.1046/j.1365-2389.2002.00429.x.

[31] A. Pierret, C. Doussan, Y. Capowiez, F. Bastardie, L. Pagès, Root functional architecture: A framework for modeling the interplay between roots and soil, Vadose Zo. J. 6 (2007) 269, http://dx.doi.org/10.2136/vzj2006.0067.

[32] X. Tian, P. Doerner, Root resource foraging: does it matter?, Front. Plant Sci. 4 (2013) http://dx.doi.org/10.3389/fpls.2013.00303.

[33] C. Guiot, N. Pugno, P.P. Delsanto, Elastomechanical model of tumor invasion, Appl. Phys. Lett. 89 (2006) 23–25, http://dx.doi.org/10.1063/1.2398910.

[34] V.D. Gordon, M.T. Valentine, M.L. Gardel, D. Andor-ardo, S. Dennison, A.A. Bogdanov, D.A. Weitz, T.S. Deisboeck, Measuring the mechanical stress induced by an expanding multicellular tumor system : a case study, Exp. Cell Res. 289 (2003) 58–66, http://dx.doi.org/10.1016/S0014-4827(03)00256-8.

[35] F. Benoist, F. Box, A. Goriely, Edge effects in elastic bulging, Int. J. Non Linear Mech. (2018).

[36] Y. Liu, Y. Ye, A. Althobaiti, Y.-X. Xie, Prevention of localized bulging in an inflated bilayer tube, Int. J. Mech. Sci. (2019).

[37] L.D. Landau, E.M. Lifshitz, Theory of Elasticity, Pergamon Press, 1970.

[38] J. Prescott, Applied Elasticity, Dover Publications, New York, 1946.

[39] A.G. Bengough, M.F. Bransby, J. Hans, S.J. McKenna, T.J. Roberts, T.A. Valentine, Root responses to soil physical conditions; growth dynamics from field to cell, J. Exp. Bot. (2006) 437–447, http://dx.doi.org/10.1093/jxb/erj003.

[40] A.G. Bengough, C. Croser, J. Pritchard, A biophysical analysis of root growth under mechanical stress, Plant Soil 189 (1997) 155–164, http://dx.doi.org/10.1023/A:1004240706284.

[41] A.R. Dexter, Mechanics of root growth, Plant Soil 98 (1987) 303–312, http://dx.doi.org/10.1007/BF02378351.

[42] L.M.A. Bettencourt, J. Lobo, D. Helbing, C. Kuhnert, G.B. West, Growth, innovation, scaling, and the pace of life in cities, Proc. Natl. Acad. Sci. 104 (2007) 7301–7306, http://dx.doi.org/10.1073/pnas.0610172104.

[43] G.B. West, J.H. Brown, B.J. Enquist, A general model for the origin of allometric scaling laws in biology, Science (80-.) (1997) http://dx.doi.org/10.1126/science.276.5309.122.

[44] G.B. West, J.H. Brown, B.J. Enquist, A general model for ontogenetic growth, Nature 413 (2001) 628–631, http://dx.doi.org/10.1038/35098076.

[45] A.G. Bengough, C.J. Mackenzie, Simultaneous measurement of root force and elongation for seedling pea roots, J. Exp. Bot. 45 (1994) 95–102, http://dx.doi.org/10.1093/jxb/45.1.95.

[46] A.G. Bengough, Root elongation is restricted by axial but not by radial pressures: So what happens in field soil?, Plant Soil 360 (2012) 15–18, http://dx.doi.org/10.1007/s11104-012-1428-8.

[47] E. Kolb, C. Hartmann, P. Genet, Radial force development during root growth measured by photoelasticity, Plant Soil 360 (2012) 19–35, http://dx.doi.org/10.1007/s11104-012-1316-2.

[48] Y. Forterre, Slow, fast and furious: Understanding the physics of plant movements, J. Exp. Bot. 64 (2013) 4745–4760, http://dx.doi.org/10.1093/jxb/ert230.

[49] B.M. Das, Advanced Soil Mechanics, fourth ed., 2014, http://dx.doi.org/10.1029/EO066i042p00714-02.

[50] J.E. Bowles, Foundation Analysis and Design, 1997, http://dx.doi.org/10.1016/0013-7952(84)90010-3.

[51] V. Normand, D.L. Lootens, E. Amici, K.P. Plucknett, P. Aymard, New insight into agarose gel mechanical properties, Biomacromolecules (2000) http://dx.doi.org/10.1021/bm005583j.

[52] A. Schiavi, R. Cuccaro, A. Troia, Strain-rate and temperature dependent material properties of Agar and Gellan Gum used in biomedical applications, J. Mech. Behav. Biomed. Mater. 53 (2016) 119–130, http://dx.doi.org/10.1016/j.jmbbm.2015.08.011.

[53] F. Baluska, D.V.M. Hauskrecht, P.W. Barlow, Root cap mucilage and extracellular calcium as modulators of cellular growth in postmitotic growth zones of the maize root apex, Bot. Acta. 109 (1996) 25–34.

Plant root penetration and growth as a mechanical inclusion problem

B. Calusi[a,b,*,], F. Tramacere[a], S. Gualtieri[a], N.M. Pugno[b,c,d,**], B. Mazzolai[a,**]**

[a]Center for Micro-BioRobotics, Istituto Italiano di Tecnologia, Viale Rinaldo Piaggio 34, 56025 Pontedera, Italy
[b]Laboratory of Bio-inspired & Graphene Nanomechanics, Department of Civil, Environmental and Mechanical Engineering, University of Trento, Via Mesiano 77, 38123 Trento, Italy
[c]Ket-Lab, Amaldi Foundation, Via del Politecnico snc, 00133 Rome, Italy
[d]School of Engineering and Materials Science, Queen Mary University of London, Mile End Road, London E1 4NS, UK
[*] **Currently at the:** Istituto Nazionale di Geofisica e Vulcanologia, Via Cesare Battisti 53, 56125 Pisa, Italy
[**] **Corresponding authors.** *E-mail addresses*: benedetta.calusi@ingv.it (B. Calusi), nicola.pugno@unitn.it (N.M. Pugno), barbara.mazzolai@iit.it (B. Mazzolai)

Supplementary material

The presented data and analyses were obtained by planting *Zea mays L.* roots in water on filter paper for 2 days and in artificial soil medium in presence of mechanical and nutrient stimuli for further 3 days at 25°C. We used scanning electron microscopy (SEM) to measure the morphology of 2-days old roots (Figure S.3.1) and root hair distribution (Figure S.3.2). Artificial soils were prepared with different Phytagel concentrations (PC) and different nutrient concentrations were obtained using Murashige and Skoog Basal Salt Mixture (MS). The data collected in artificial soils include (1) growth measurements and statistical analysis due to the influence of increasing Phytagel concentration to increase the mechanical impedance during the growth (Table S.4.1 and Table S.4.2); (2) growth measurements and statistical analysis due to an excessive nutrient concentration into the growing medium (Table S.4.3, Table S.4.4, and Table S.4.5). In the latter case, images of longitudinal sections of the swelling of the root apical zone are provided (Figure S.3.3).

S.1. Supplementary Methods

S.1.1. Experiments design

S.1.1.1. Planting

Seeds of *Zea mays L.* were sterilized in 80% ethanol for 3 minutes and then two times in 50% bleach solution (15 minutes for each time). After five rinses in sterile Millipore water, the seeds were placed on sterile filter paper into a dark growth chamber (25 ºC) for the germination. After 2 days, roots of 1.5 cm length were selected, transplanted into the artificial soil has to be tested and placed into a growth chamber with a photoperiod of 15 h of light (25 ºC).

S.1.1.2. Artificial soils – Physical and chemical stimuli

In order to test the influence of the soil hardness and nutrient availability in the root morphology and growth kinetics, two types of experiments were carried out. In both the two cases, the plant samples were prepared

1

as described in the previous Subsection and were placed into a plastic cylinder tubes of 3 cm diameter, where previously were poured the artificial soil has to be tested.

In the first experiment, different soil compactions were obtained modifying the concentration of gel used as artificial soil. Five artificial soils were prepared using 0.15, 0.3, 0.6, 0.9, and 1.2% of Phytagel concentration, respectively. Phytagel (Sigma, Co.) is a common gelling agent used in plant culture practice; since high transparency, it allows to easily check and visualize the roots during the entire experiment. The approach used was to prepare media with increasing concentration of gel but without nutrients. Preliminary experiments were carried out to test the different concentrations of the gel to obtain strong, homogeneous and repeatable growth media; in fact, a high quantity of the Phytagel produces suspensions to much viscous and, for our experimental protocol, it was not possible to obtain gels stronger than 2%. The final gels concentrations used for the experiments were the following: 0.15, 0.30, 0.60, 0.90 and 1.2%; gels higher than 1.2% were excluded because during the preparation we observed non-homogeneous distributions of the materials after cooling.

To obtain a complete and precise indication of the mechanical strength values at various concentrations, we tested the gels by means of uniaxial unconfined compression test. This method is largely applied to test the stiffness of gels or emulsions in the food industry, but also in literature is used for the characterization of hydrogels and gels [1]. The Young modulus of each soil was measured by means of Instron 4464 (1mm/min testing speed and 5 mm displacement). We registered a maximum value of strength 80.9 KPa (correspond to 1.2% Phytagel) and the final root length of seedlings grown in these media suggests like the root seems to be stimulated in elongation respect to the lower hardness.

In the second experiment, the samples were placed into soils with different nutrients availabilities. According to the protocol described by Murashige and Skoog [2], four different nutrients concentrations of MS (Murashige and Skoog Basal Salt Mixture, Sigma, Co.) were prepared at ph 5.8: MS1, MS2, MS3, and MS4 with 0.215, 0.43, 0.86, and 1.72% MS concentration (w/v), respectively. The experiments were repeated for three different Phytagel concentrations: 0.3, 0.6, 0.9%.

S.1.2. Microscopical analysis

Plants were carefully removed from the plastic tubes and then observed with Hirox (Digital microscope - KH7700). The total length of root, top diameter, apex diameter, and hairless area were measured.

In order to deeply investigate the root morphology, some samples (N=5) were studied by means of SEM (Scanning electron microscopy, Helios NanoLab 600i, FEI). In this case, the samples were fixed in 70% ethanol and then were dried by using a critical point drying apparatus (Supercritical Autosamdri, 931.GL-Tousimis). Dried samples were mounted on aluminum stubs and sputter coated with a 5 nm thick layer of gold (Leybold DC Sputtering, Sistec).

2

Moreover, longitudinal sections of root were analyzed by means of SEM and inverted optical microscope (Nikon Eclipse Ti). In this case, the terminal portion (10 mm) of some plant roots (N=15) were excised. The samples obtained were fixed in a solution of 4% Paraformaldehyde, dehydrated first through a graded series of ethanol (30%, 50%, 70%, 85%, 95%, and 100 %) and then through a graded series of xylene (25%, 50%, 75%, and 100%). Later, the samples were included in paraffin and cut by means of a microtome (Sliding Microtome SM2010R, Leica).

For SEM analysis, longitudinal sections with 10 μm thickness, was mounted on a special slide and then covered with gold (5nm) (Leybold DC Sputtering, Sistec).

For inverted optical microscope (Nikon Eclipse Ti), a longitudinal section with 5 μm thickness was stained with 1% methylene blue for 5 minutes and then mounted with BioMount HM (Bio-Optica). The images of sections were obtained with a CCD camera (DS-5MC USB2, Nikon).

S.2. Supplementary Data Analysis

S.2.1. Gross root morphology and kinetics in water

The morphology of two days old primary root of *Zea mays L.* has been studied by means of scanning electron microscopy (SEM). The root has a total length and a diameter at the base of the seed (called top diameter in the rest of this work, please refer to Figure S.3.2) of 16±5 mm and 1.25±0.07 mm, respectively. The samples, due to the drying process needed for SEM analysis, have shown a size reduction of 0.25% and 5%, respect to the physiological conditions, in length and top diameter, respectively. The plants grown in sterile Millipore water, show a root entirely covered by a dense network of hairs (13 μm diameter), except for the terminal part (apical part) that is instead completely hairless (called hairless area in the rest of this work, please refer to Figure S.3.2) (Figure S.3.1a-b). In 2-days old roots, the hairless area extends almost for 3 mm length (including meristematic and elongation region) and root diameter 3 mm above the tip (called apex diameter in the rest of this work, please refer to Figure S.3.2) is 1.11±0.04 mm. The growth kinetics has been monitored for 6 days age (we analyzed N=39, 27, 28, 30 samples at 3, 4, 5, and 6 days since germination, respectively). The total root length has shown a growth rate of 28.3 mm/day, the top diameter has been almost constant (1.26±0.08 mm), the hairless area has significantly increased until has covered the entire root length at 6-day age (no presence of root hairs); meanwhile the apex diameter has decreased of 26% respect to the value at 2-day age.

S.2.2. Physical stimulus – Soil hardness

The influence of soil hardness has been evaluated using the same artificial soil with five different Phytagel concentrations. Total length, top diameter, and apex diameter have been measured at 3, 4, 5, and 6 days since germination (Table S.4.1). A different growth rate has been observed increasing the soil hardness:

3

18.7, 21.8, 21.9, 22.9, and 23.4 mm/day have been found for 0.12, 0.3, 0.6, 0.9, and 1.2% Phytagel concentration, respectively. ANOVA analysis results are reported in Table S.4.2.

S.2.3. Chemical stimulus – Nutrients availability

The influence of nutrients availability has been evaluated using four different concentrations of MS medium dissolved in artificial soils. In this case, the soil hardness has been kept constant. In order to be sure that soil hardness does not influence the plant behavior, the experiment has been repeated for three different soil hardnesses (0.3, 0.6, and 0.9% Phytagel concentration). Measurements of length and top diameter were carried out at 3, 4, 5, and 6 days since germination. The growth rate and the root length and thickness are reported in Table S.4.3 and Table S.4.4. ANOVA analysis was used and reported in Table S.4.5. To investigate swelling of diameter in the apical zone of the primary root, longitudinal histological sections of root presenting this morphological feature have been carried out. This morphological feature has been found only in 5-6 days old plants growth in soil with a MS4 of nutrients concentration. This swelling has been observed at the height of the elongation zone and presents a diameter 17% thicker than mature region diameter (generally, the diameter in the elongation zone is 43% smaller than the diameter in the mature zone). In Figure S.3.3, a general swelling of the apex is evident due to a transverse and radial enlargement of cells in stele tissues. Also, an irregular cellular division in the cortex has been shown, respect to the isodiametric and ordered cells in the control plants (Figure S.3.3).

S.3. Supplementary Figures
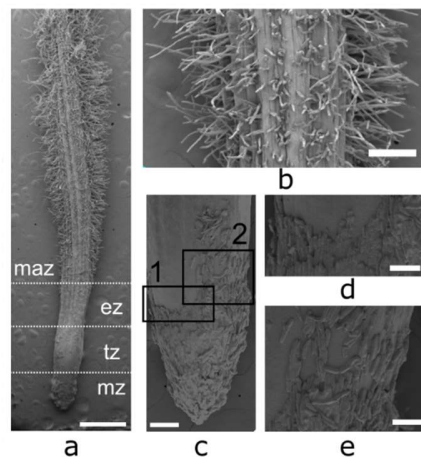
Figure S.3.1: SEM images of 2 days old *Z. mays* root. a) Root structure. maz, mature zone; ez, elongation zone; tz, transitional zone; and mz, meristematic zone. The scale bar equals 1 mm. b) Root hairs, present in the mature zone. The scale bar equals 200μm. c) Root apex characterized by root cap and sloughing cells. The scale bar equals 200 μm. d-e) Enlargement of black boxes in (c). The scale bar equals 100 μm.
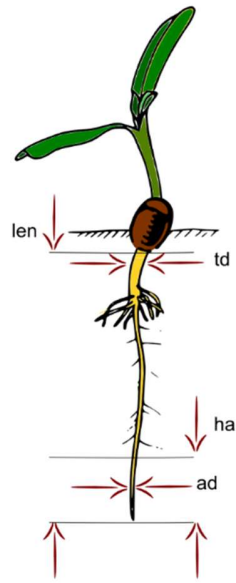
Figure S.3.2: Gross structure of shoot. len, root total length; td, top diameter; ad, apex diameter; and ha, hairless area.
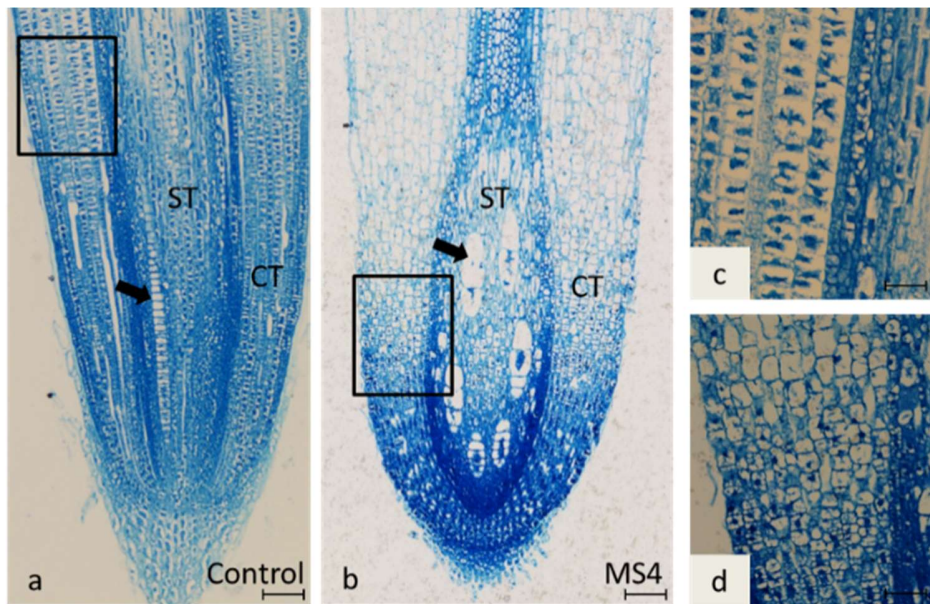
Figure S.3.3: Light microscopy images. Longitudinal sections of six days old maize root tips grown in air (control) and under high concentration of nutrients (MS4). The black rectangular frames in (a) and (b) indicate cortex tissue detail observed in (c) and (d), respectively. In (c) are visible the cortex cells that appear isodiametric and uniformly placed; differently, in the stressed roots (d), the cells are irregular. The arrows indicate the enlargement observed in stele tissues in plants under high concentrations of nutrients (b) and the normal development in control samples. CT = cortex tissue; ST = stele tissue. Bar = 200 µm.

S.4. Supplementary Tables

Soil	Measurements (mm)	Day 3	Day 4	Day 5	Day 6
0.15% PC	**L**	43.88±10.56	61.50±5.76	100.06±10.37	122.06±13.07
	$\varnothing_{seed}$	1.28±0.09	1.36±0.09	1.43±0.06	1.34±0.11
	$\varnothing_{apex}$	1.08±0.10	1.05±0.04	1.05±0.04	0.99±0.07
	N	8	8	16	16
0.3% PC	**L**	50.25±10.71	85.88±14.55	111.31±8.96	137.79±16.21
	$\varnothing_{seed}$	1.41±0.11	1.36±0.09	1.37±0.06	1.36±0.08
	$\varnothing_{apex}$	1.21±0.07	1.09±0.04	0.99±0.04	0.96±0.07
	N	8	8	16	19
0.6% PC	**L**	61.88±12.38	89.38±15.07	111.06±13.00	130.50±16.05
	$\varnothing_{seed}$	1.39±0.12	1.36±0.09	1.41±0.11	1.35±0.07
	$\varnothing_{apex}$	1.19±0.14	1.21±0.03	1.08±0.06	0.97±0.05
	N	8	8	17	18
0.9% PC	**L**	61.50±5.76	85.00±14.14	112.50±9.95	146.62±9.36
	$\varnothing_{seed}$	1.38±0.10	1.34±0.09	1.37±0.10	1.38±0.08
	$\varnothing_{apex}$	1.17±0.09	1.07±0.04	0.98±0.03	0.90±0.06
	N	8	8	14	13
1.2% PC	**L**	45.60±8.32	80.30±13.56	118.40±5.42	159.70±9.53
	$\varnothing_{seed}$	1.46±0.08	1.47±0.05	1.51±0.10	1.50±0.08
	$\varnothing_{apex}$	1.23±0.10	1.07±0.03	1.08±0.07	0.96±0.05
	N	10	10	10	10

Table S.4.1: Length, top diameter, apex diameter (mean±SD) of the primary root, and the number of measurements, considering five different soil hardness corresponding to different Phytagel concentrations (PC).

Day	Measurements	ANOVA parameters df_{TOT}	df_{AMONG}	F	p
3	**L**	57	6	5.83	0.0001
	$\varnothing_{seed}$	57	6	5.13	0.0003
	$\varnothing_{apex}$	57	6	6.16	<<0.0001
4	**L**	57	6	4.66	0.0008
	$\varnothing_{seed}$	57	6	4.78	0.0006
	$\varnothing_{apex}$	57	6	22.25	<<0.0001
5	**L**	88	6	4.98	0.0002
	$\varnothing_{seed}$	88	6	3.83	0.002
	$\varnothing_{apex}$	88	6	47.85	0
6	**L**	91	6	12.41	<<0.0001
	$\varnothing_{seed}$	91	6	7.62	<<0.0001
	$\varnothing_{apex}$	91	6	21.3	<<0.0001

Table S.4.2: ANOVA analysis of root features gathered in Table S.4.1 (df_{TOT}, total group degrees of freedom; df_{AMONG}, among group degrees of freedom; F, F-test of Fisher; p, p-value).

	Group MS1		Group MS2		Group MS3		Group MS4	
Day	L	Ø	L	Ø	L	Ø	L	Ø
0.3% PC								
3	28.9±9.4	1.5±0.1	30.0±3.3	1.4±0.1	30.0±1.4	1.6±0.0	16.0±6.9	1.2±0.1
	N = 7		N = 4		N = 5		N = 8	
4	70.0±16.1	1.6±0.1	62.5±8.1	1.4±0.1	49.3±11.1	1.5±0.1	37.3±4.2	1.4±0.1
	N = 7		N = 6		N = 8		N = 8	
5	84.6±13.0	1.5±0.1	87.5±10.4	1.4±0.1	64.4±14.2	1.4±0.1	39.1±5.5	1.4±0.1
	N = 17		N = 16		N = 16		N = 17	
6	117.9±12.5	1.0±0.3	109.3±7.9	1.4±0.1	84.3±14.0	1.3±0.1	46.3±3.5	1.5±0.1
	N = 7		N = 7		N = 7		N = 8	
0.6% PC								
3	40.4±11.0	1.5±0.1	46.9±5.9	1.4±0.1	40.8±3.8	1.5±0.1	26.2±6.6	1.6±0.1
	N = 8		N = 8		N = 6		N = 8	
4	72.0±6.8	1.4±0.0	69.3±4.6	1.4±0.1	52.0±15.9	1.4±0.1	40.5±2.3	1.6±0.1
	N = 8		N = 7		N = 6		N = 6	
5	97.9±9.0	1.4±0.1	93.0±6.0	1.4±0.1	84.0±4.9	1.4±0.1	42.9±9.5	1.5±0.1
	N = 8		N = 8		N = 8		N = 7	
6	108.3±13.5	1.4±0.1	100.3±11.6	1.5±0.1	90.3±10.8	1.4±0.1	46.1±14.3	1.5±0.1
	N = 16		N = 16		N = 16		N = 17	
0.9% PC								
3	46.4±4.6	1.4±0.1	44.4±5.4	1.5±0.1	43.1±6.1	1.4±0.1	25.8±5.0	1.5±0.1
	N = 16		N = 14		N = 15		N = 16	
4	64.7±8.3	1.4±0.1	63.5±8.1	1.5±0.1	58.1±11.4	1.5±0.1	38.9±5.8	1.5±0.1
	N = 15		N = 15		N = 16		N = 13	
5	97.9±4.6	1.4±0.1	92.7±6.5	1.4±0.1	72.7±9.3	1.4±0.1	50.4±3.9	1.4±0.1
	N = 15		N = 15		N = 15		N = 15	
6	122.8±6.7	1.3±0.0	106.9±7.7	1.5±0.1	91.2±10.7	1.5±0.1	65.6±3.9	1.5±0.1
	N = 8		N = 7		N = 6		N = 8	

Table S.4.3: Length and top diameter (mean±s.d. (mm)) considering four different nutrient concentrations (MS1, MS2, MS3, and MS4) and the corresponding measurements. The experiments were carried out for three different soil hardnesses (0.3, 0.6, and 0.9% Phytagel concentration, PC).

	Group MS1	Group MS2	Group MS3	Group MS4
0.3% PC	17.4	16.7	13.0	7.8
0.6% PC	18.0	17.3	15.0	8.5
0.9% PC	18.9	17.3	14.8	10.2

Table S.4.4: Growth rate (mm day^{-1}) of roots in different soil hardnesses. (0.3, 0.6, and 0.9% Phytagel concentration) and nutrient concentrations (MS1, MS2, MS3, and MS4 nutrient concentration). PC is the Phytagel concentration.

	Day 3		Day 4		Day 5		Day 6	
	L	**Ø**	**L**	**Ø**	**L**	**Ø**	**L**	**Ø**
0.3% PC								
df$_{TOT}$	23	23	28	28	65	65	28	28
df$_{AMONG}$	3	3	3	3	3	3	3	3
F	7.23	27.69	13.46	3.98	66.22	1.12	75.95	8.03
p	<< 0.01	<< 0.01	<< 0.01	<< 0.05	<< 0.01	0.35	<< 0.01	<< 0.01
0.6% PC								
df$_{TOT}$	29	29	26	26	30	30	64	64
df$_{AMONG}$	3	3	3	3	3	3	3	3
F	10.74	3.01	19.33	5.4	79.97	9.58	80.47	0.36
p	<< 0.01	< 0.05	<< 0.01	< 0.01	<< 0.01	<< 0.01	<< 0.01	0.78
0.9% PC								
df$_{TOT}$	60	60	58	58	59	59	28	28
df$_{AMONG}$	3	3	3	3	3	3	3	3
F	51.23	5.63	25.03	5.35	171.33	0.84	87.89	5.44
p	<< 0.01	<< 0.01	<< 0.01	< 0.01	<< 0.01	0.48	<< 0.01	< 0.01

Table S.4.5: ANOVA analysis of root features gathered in Table S.4.3 (dfTOT, total group degrees of freedom; dfAMONG, among group degrees of freedom; F, F-test of Fisher; p, p-value). PC is the Phytagel concentration.

References

[1]   C. Yamamoto, Y. Sakata, T. Taji, T. Baba, S. Tanaka, Unique ethylene-regulated touch responses of arabidopsis thaliana roots to physical hardness, J. Plant Res. 121 (2008) 509–519. doi:10.1007/s10265-008-0178-4.

[2]   A. Pierret, C. Doussan, Y. Capowiez, F. Bastardie, L. Pagès, Root Functional Architecture: A Framework for Modeling the Interplay between Roots and Soil, Vadose Zo. J. 6 (2007) 269. doi:10.2136/vzj2006.0067.